Growth of Non-enzymatic Cholesterol Biosensor using TiO_2 Decorated Graphene Oxide with Bare GCE and PPy-GCE

S. DEIVANAYAKI[1*], P. JAYAMURUGAN[2], S. ASHOKAN[3], V. GOPALA KRISHNAN[4] AND B. YOGESWARI[5]

[1]Department of Physics, Sri Ramakrishna Engineering College, Vattamalaipalayam, Coimbatore-641022, Tamil Nadu, India.

[2]Department of Physics, Sri Ramakrishna Mission Vidyalaya College of Arts and Science, Coimbatore-641020, Tamil Nadu, India.

[3]Department of Physics,Bannari Amman Institute of Technology, Sathymangalam, Erode-638401,Tamil Nadu, India.

[4]Department of Physics, Dr. N. G. P. Arts and Science College Coimbatore- 641048 Tamil Nadu, India.

[5]Department of Physics, Sri Eshwar College of Engineering, Coimbatore-641202, Tamil Nadu, India.

ABSTRACT

The cholesterol level determination is a significant clinical diagnostic solution for heart and, thrombosis problems. In this work, we examined a novel non-enzymatic cholesterol biosensor using cholesterol oxidase (ChOx) enzyme immobilized on TiO_2 nanoparticles influenced by reduced graphene oxide (rGO) - polypyrrole (PPy) (rGO-TiO_2/PPy-GCE) nanocomposite was developed on a glassy carbon electrode (GCE) and the higher sensing response with lower detection limits were observed. The electrochemical properties of GCE modified PPy (PPy-GCE) were studied using CV (Cyclic Voltammetry) and DPV (Differential Pulse Voltammetry). The reported sensor exhibited piecewise linearity in the range of 0.1 µM to 1 µM and 1 µM to 600 µM with the sensing response of 61.665 and 0.1466 (2µA µM×cm) respectively. The detection limits of the sensor were found to be 32 nm. The results were repeatable and reproducible and this sensor can be applied to determine the cholesterol at real sample with satisfactory results.

KEYWORDS: *Clinical analysis, Non-enzymatic, Nanomaterials, Chemical oxidative polymerisation*

J. Polym. Mater. Vol. **38,** No. 3-4, 2021, 295-307

Correspondence author e-mail: deivasrinath@gmail.com
DOI : https://doi.org/10.32381/JPM.2021.38.3-4.10

1. INTRODUCTION

Cholesterol and other fatty acids are important components of the human body. Cholesterol helps the body make cell membranes, many hormones, and vitamin D. Cholesterol comes from food and the liver. Cholesterol and other fats are carried in the bloodstream as spherical particles (ie., lipoproteins)[1]. The normal total cholesterol level in healthy human serum is approximately 200 mg dl (or 5.17 mM)[2, 3]. Estimation of cholesterol levels is extremely important for clinical diagnosis. Different approaches, including high performance liquid chromatography[4-7], near infrared (IR) spectra[8-10] and colorimetric assay[11-13], have been used to detect cholesterol levels. However, the above approaches are expensive and time consuming and require large amounts of serum samples[14]. Therefore, a rapid, robust and sensitive cholesterol detection method must be developed.

Among these methods, electrochemical detection has attracted and considerable attention because of its speed, simplicity, and low cost. Most of the literature on electrochemical based cholesterol sensors has focused on determination based on the activity of the enzyme "cholesterol oxidase"[15]. Alagappa et al.,[16] reported an electrochemical cholesterol biosensor based on cholesterol oxidase (ChOx) enzyme immobilized on gold nanoparticles – functionalized – multiwalled carbon nanotube (MWCNT) – polypyrrole (PPy) nanocomposite modified electrode. The sensor was fabricated by a two-step approach wherein the Au NPs-f-MWCNT was prepared by wet chemical method followed by electro polymerization of pyrrole. The AuNPs-f-MWCNT-PPy-ChOx/GCE showed a linear response from 2×10^{-3} to 8×10^{-3}/M in amperometry with a sensitivity and detection limit of 10.12/μA/mM^{-1} cm^{-3} and 0.1×10^{-3}/M respectively. Ansari et al.[17] studied the CHIT–tin oxide (SnO_2) nano-biocomposite film for cholesterol biosensor development. They showed that ChOx/CHIT-SnO_2/ITO (Indium–Tin–Oxide) was more stable than the ChOx/CHIT/ITO bioelectrode, and it presented a high sensitivity of 34.7mA/mg$dL^{-1}cm^2$, a linear response in the range of 10–400mg/dL, and a low detection limit of 5mg/dL. Nguyet et al.[18] reported a DNA sensor based on the CeO_2/PPy nanocomposite for Salmonella detection. In situ chemical oxidative polymerization was used to prepare the core–shell CeO_2-NR@PPy nanocomposite, which provided a suitable platform for electrochemical DNA biosensor fabrication. The sDNA/CeO_2NRs@PPy/electrode response under optimal conditions presented a linearity between 0.01 and 0.4nM with a sensitivity of 593.7Ω•nM^{-1}•cm^{-2}.Tiwari and Gong[19] reported a novel chitosan (CHIT)/SiO_2/multiwalled carbon nanotube (MWCNT)/electrode-based cholesterol biosensor. They established the linear relationship between oxidation current response and cholesterol concentrations to be in the range of 5.0–5000 μg/mL, a response time of 5s, and a sensitivity of 3.4nA/mg dL^{-1}. Wisitsoraat et al.,[20] developed a new cholesterol biosensor by using carbon nanotubes (CNT) directly growth on a glass-based chip via the low-temperature chemical vapor deposition process. They determined the linear detection range to be between 50 and 400mg/dL with a sensitivity of 0.0512nA/mg•dL^{-1}.

Among the metal oxide NPs based biosensor, the interest for titanium dioxide (TiO_2) NPs is

being attention due to its unique properties such as high surface area and high catalytic efficiency, which can improve the interaction between biomolecules and electrode surfaces [21–25]. Recently, cholesterol bio-sensor based on TiO_2 nanotubes decorated with Cu_2O nanoparticles has been reported[26]. Particularly, reduced graphene oxide performed cholesterol oxidase (ChOx) exhibits fast response and repeatable cyclic process in sensor[27] and also the polypyrrole (PPy) influenced electrochemical sensor shows flexibility, better electrical conductivity and surface characteristics[28]. Meanwhile, electrode influences is the important parameter in sensor, a lot of work were mentioned[16-20] with different electrode but the higher efficiency with fast responded electrode of glassy carbon electrode was not preferred. The merits of the biosensor using TiO_2 nanoparticles, reduced graphene oxide (rGO), polypyrrole (PPy) developed on glassy carbon electrode (GCE) was reported as many but the compositional work using glassy carbon electrode (GCE) and their sensing response was not reported on literature survey.

In the present work, a novel biosensor based on the cholesterol oxidase (ChOx) enzyme immobilized on TiO_2 nanoparticles influenced by reduced graphene oxide (rGO)/polypyrrole (PPy) (rGO-TiO_2/PPy-GCE) nanocomposite was developed on a glassy carbon electrode (GCE).

2. EXPERIMENTAL AND MATERIAL CHARACTERIZATION

2.1 Reagents and Sample Preparation

All the chemicals were used analytical grade. Cholesterol, Triton X-100 & IPA, diethyl ether, petroleum, hydrogen peroxide, potassium permanganate, sulphuric acid, hydrochloric acid, potassium ferricyanide ($K_3[Fe(CN)_6]$), sodium hydroxide pellets, potassium dihydrogen orthophosphate (KH_2PO_4) and acetone were bought from Loba chemie. Ethanol was brought from Changshu Yanguan Chemical Ltd., Ultrapure water (MilliQ, Millipore water) was used for all the experiments. Since cholesterol is not soluble in aqueous media, stock solutions were prepared by dissolving cholesterol initially in Triton X-100 and then suitable solvents (0.1 M NaOH or PBS) were added. The composition of the solutions used will be explained in the respective sections.

Graphene oxide (GO) was synthesized directly from graphite by the Hummers method. The rGO and rGO-TiO_2 nanocomposites synthesis was assisted by hydrothermal process. Nanocomposites rGO-TiO_2/PPy was synthesized by in-situ chemical oxidative polymerization technique. A bare glassy carbon electrode (GCE) or a modified GCE was applied as the working electrode, meanwhile, a saturated calomel electrode (SCE) and a platinum wire were used as the reference and counter electrodes, respectively.

The aliquot of cholesterol was extracted from egg yolk for the real sample analysis to evaluate the sensor performance. The yellow yolk portion of egg is removed separately, washed and filtered to remove other contents. A small puncture was made in the slaggy yolk and pure yolk was taken for the further electrochemical analysis. 10 g of egg yolk was weighed and then diluted to 50 mL using distilled water. 5 mL of aliquot was mixed thoroughly with 5 mL of IPA, 12.5 mL diethyl ether and 12.5 mL of petroleum ether in a separating funnel. The mixture was shaken well and the inorganic layer was separated from the organic layer. The organic layer was separated and the organic solvents were allowed to evaporate.

2.2 Material Characterization

The prepared samples were characterized by Scanning electron microscopy (SEM, Hitachi S-4800), Fourier transform infrared spectroscopy (FT-IR-8700 spectrometer), UV-Visible spectroscopy (JASCO V-530) and Thermal gravimetric analysis (NETZSCH STA 2500).

All electrochemical experiments were performed on a CHI 920C electrochemical workstation (SREC, Coimbatore) with a conventional three-electrode system.The electrode was standardized by performing Cyclic voltammetry (CV) in 1 mM of potassium ferricyanide ($K_3[Fe(CN)_6]$) and 100 mM of potassium chloride (KCl) as supporting electrolyte with initial and final potential of -0.25 V to +0.5 V respectively and the scan rate of 50 mV/s. Ferulic acid was sensed using CV and differential pulse voltammetry (DPV) with the presence of some concentration of ferulic acid in phosphate buffer. The CV parameters for detection of ferulic acid were -0.3 V to 0.9 V with the scan rate of 50 mV/s, the DPV parameters were 0 to 1.5 V as initial and final potential, 0.05 V as pulse increment. The electrode was modified and standardized after each electrochemical measurement.

3. RESULTS AND DISCUSSIONS

3.1 Functional Group Analysis of GO, rGO and rGO-TiO_2

Graphene oxide (GO), reduced graphene oxide (rGO) and TiO_2 decorated graphene oxide (rGO-TiO_2) were characterized for their presence of functional groups using FT-IR spectroscopy. Fig. 1 shows the obtained FT-IR spectra for GO, rGO and rGO-TiO_2. The absorption band near 522 cm^{-1} corresponded to the Ti-O vibration[29]. The peak strength of rGO-TiO_2 nanocomposites is lower than GO and some of the peaks even disappear. From the FT-IR spectrum of rGO-TiO_2 nanocomposites, few peaks indicating the

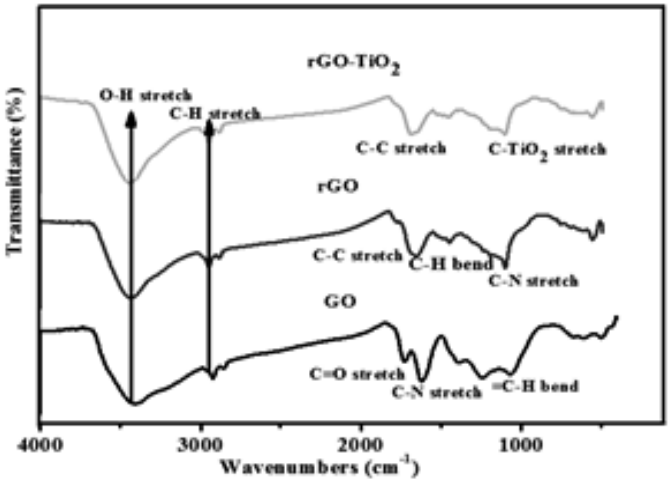

Figure 1. FT-IR spectra of GO, rGO and rGO-TiO_2

oxygen containing functional groups can be seen after reduction. These oxygen-containing functional groups demonstrate the successful preparation of GO and provide anchoring sites for the adsorption of heavy metal ions on the TiO_2/GO-8 nanocomposites[30]. The FT-IR spectra of raw and coated fabrics displayed a broad absorption band of around 3285cm^{-1}, which is attributed to the O–H stretching vibration of C–OH groups[31]. GO exhibited functional groups like –OH, –COOH, C=O whereas rGO exhibited reduced levels of –OH and negligible amount of C=O stretch which results in enhanced conductivity. The spectra

of rGO-TiO_2 exhibit the presence of TiO_2 in the form of C-TiO_2 functional group which confirmed the formation of TiO_2 nanoparticles.

3.2 Absorption Spectra of GO, rGO and rGO-TiO_2

UV-Vis spectra of GO, rGO and rGO-TiO_2 is presented in Fig. 2. UV-Vis spectrum of GO exhibits the absorption at 230 nm which is due to p-p*transition[32]. The spectrum for rGO exhibits the absorption at the shifted wavelength of 260 nm compared to GO. Fig shows rGO-TiO_2 exhibits the absorption for rGO at 260 nm and an another absorption peak at 350 nm which corresponds to the presence of TiO_2 [33]. The absorption of reduced graphene shifts from 226 to 256 nm, suggesting that the electronic conjugation within graphene sheets is restored after the reduction[34].

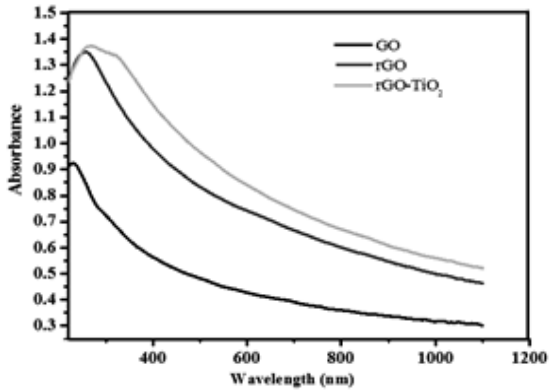

Figure 2. UV-visible spectrum for GO, rGO, rGO-TiO_2

3.3 Thermo Gravimetric Analysis of GO, rGO and rGO-TiO_2

Thermo gravimetric analysis (TGA) helps to know the weight decomposition of the sample with respect to the increase in temperature. TGA plot (Fig. 3) gives the information about the amount of the material loss with respect to the temperature.

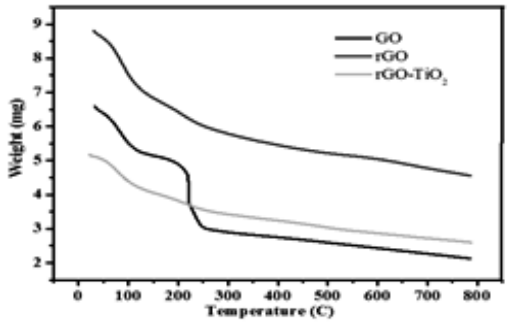

Figure 3. TGA analysis of GO, rGO and rGO-TiO_2

GO sample taken for TGA was of weight 6.5870 mg where with increase in temperature, at temperature 210°C there is decomposition occurring amounting to 54.90 % of loss which is equivalent to 3.616 mg and from temperatures 260°C to 800°C the decomposition amounts to 12.80% which is 0.8429 mg of weight. TGA plot of rGO exhibits the decomposition of 48.27% with the weight loss of 4.29 mg from the temperature 50°C to 800°C. TGA plot of rGO-TiO_2 exhibits the decomposition of 49.64% with the weight loss of 2.567 mg from 50°C to 800°C.

3.4 Surface Analysis of rGO-TiO_2

The surface morphology and topology of rGO-TiO_2 nanocomposite was characterized using SEM. Fig. 4 shows the clusters of TiO_2 nanoparticles decorated on the reduced graphene sheets. The formation of the nanoparticles is merely spherical in shape with the size of approximately 135 nm. Thus it is confirmed that TiO_2 decorated rGO has enhanced surface area and enhanced conductivity.

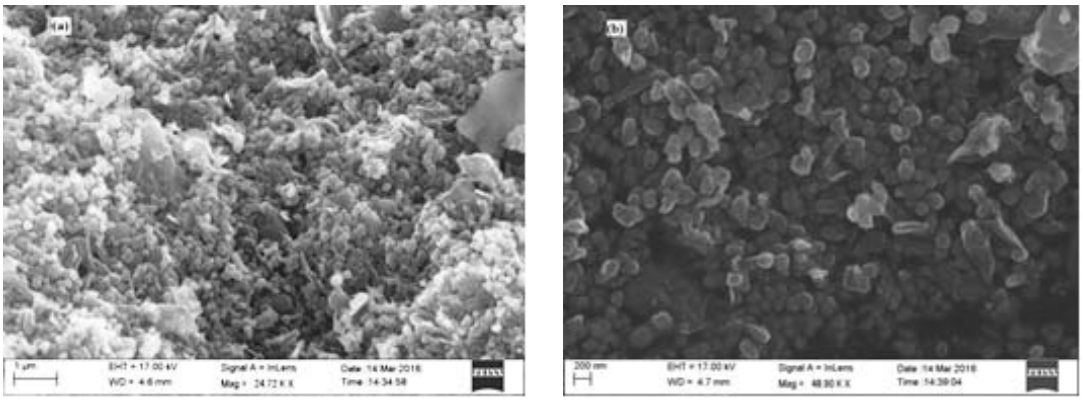

Figure 4. SEM image of (a) 1 µm and (b) 200 nm rGO-TiO_2

3.5 Calculation of Effective Surface Area

Electrochemically active area of modified electrode was calculated by performing chronocoulometry for $K_3[Fe(CN)_6]$. The Cottrell charge plot for bare electrode and modified electrode is shown in Fig. 5 which confirms the increase in electrochemically active surface area. The surface area is calculated using Cottrell equation.

$$Slope = \frac{2nFAC\sqrt{D}}{\sqrt{\pi}}$$

By substituting the known values, the surface area of the PPy modified GCE was $0.262*10^{-4}$ m^2 which is enhanced compared to the surface area of bare GCE which was of $0.196*10^{-4}m^2$. The diffusion co-efficient for bare GCE was $0.430*10^{-2}$ m^2/s.

3.6 Catalytic Activity of Modified Electrode

The catalytic activity of modified electrode was exhibited by performing Cyclic voltammetry with 1mM of $K_3[Fe(CN)_6]$ as redox species and 100 mM of KCl as the supporting electrolyte.

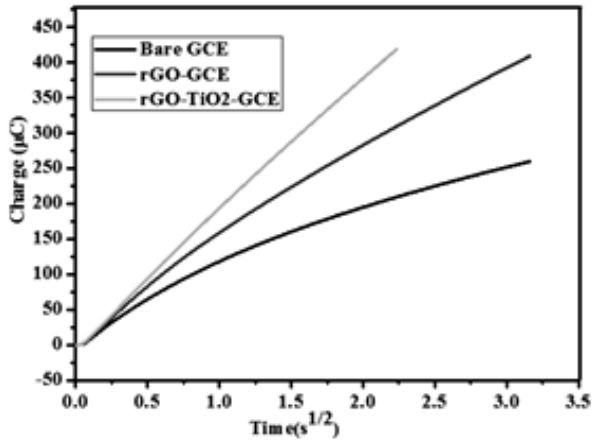

Figure 5. Chronoamperometry for bare GCE, rGO/GCE and rGO-TiO_2/GCE

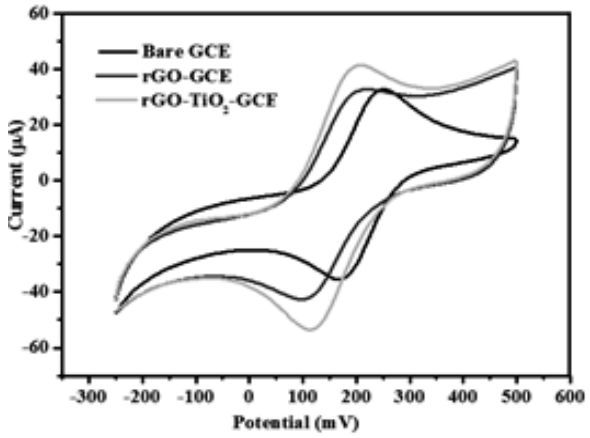

Figure 6. Cyclic Voltammogram for bare GCE, rGO/GCE, rGO-TiO_2/GCE

On performing CV for potassium ferricyanide, it results in one electron redox transfer Fig. 6 exhibits redox curve for potassium ferricyanide, the oxidation occurred at +259 mV and reduction occurred at +168 mV. In order to get better conductivity, the catalytic activity of the PPy-GCE is shown in Fig. 6 where there is increase in current and also left shift in reduction and oxidation potential compared to bare GCE. This confirms the enhanced surface area for modified electrode which helps in the increase of conductivity and sensitivity of the electrode. The peak separation potential for redox species on bare GCE was 88 mV whereas for rGO/PPy-GCE it was 95 mV and for rGO-TiO_2/PPy-GCE it was 86 mV. Catalytic activity of bare GCE, rGO/PPy-GCE and rGO-TiO_2/PPy-GCE in terms of anodic potential, cathodic potential and area under the curve are shown in the table.1

TABLE 1. Catalytic activity of bare GCE, rGO/PPy-GCE and rGO-TiO_2/PPy-GCE in terms of anodic and cathodic potential and area under the curve

Electrode	Area under the curve		Peak potential	
	Cathodic	Anodic	Anodic	Cathodic
Bare GCE	5.901 µW	15.31 µW	165 mV	253 mV
rGO/PPy-GCE	10.912 µW	11.620 µW	114 mV	209 mV
rGO-TiO_2/PPy-GCE	12.494 µW	14.057 µW	116 mV	202 mV

3.7 Optimization

Buffer used for the detection and quantification of cholestrol is phosphate buffer. The effect of pH in the buffer is studied by varying pH from 4.5 to 11.5.

Fig. 7 gives the effect of pH in the detection of cholestrol. It is evident that the pH of 7.45 is more suitable for the detection of cholestrol with maximum current response compared to other pH values.

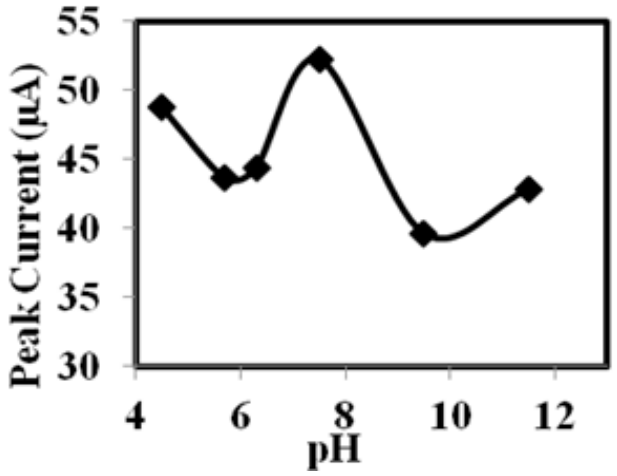

Figure 7. Calibration plot for the detection of cholestrol with various phosphate buffer

3.8 Scan Rate Variation and Detection of Cholestrol

CV was performed by varying the scanrates for the detection of cholestrol from 1 mV/s to 500 mV/s. From Fig. 8 it is observed that with increase in scan rate, there is linear increase in current response. The detection of cholestrol on bare GCE and rGO-TiO_2/PPy-GCE was done using cyclic voltammetry. Fig. 9 exhibits the cyclic voltammogram of 100 µM cholestrol and the oxidation peak was observed at 0.685 V for bare GCE and 0.619 V for rGO-TiO_2/PPy-GCE. This shows that the modified electrode shows better sensitivity and conductivity for the detection of cholestrol.

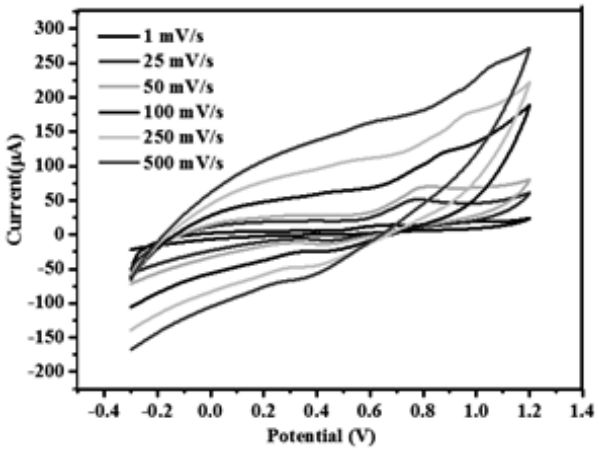

Figure 8. Cyclic voltammograms for detection of 100 uM cholestrol in optimized phosphate buffer

3.9 Linear Range and Limit of Detection

In order to detect the cholestrol of lower concentrations with high sensitivity and differential pulse voltammetry (DPV) was used as a technique for detection of cholestrol. The DPV parameters were optimized such that sharp oxidation peak was obtained with the presence of ferulic acid.

Figure 10 shows the differential pulse voltammograms for various concentrations from 0.1 μM to 600 μM. The PPy modified GCE exhibited piecewise linear range for the cholestrol detection from 0.1 μM to 1 μM ($y = 12.108x + 25.71$, $R^2 = 0.9908$) and 1 μM to 600 μM ($y = 0.0288x + 39.049$, $R^2 = 0.9798$) (Fig. 11). The sensitivity was calculated for 0.1 μM to 1 μM and 1 μM to 600 μM was 61.665 and 0.1466 respectively. The limit of quantification (LoQ) of Cholestrol for the rGO-TiO_2/PPy-GCE was found to be 0.1 μM. The limit of detection (LoD) of Cholestrol for rGO-TiO_2/PPy-GCE was found to be 0.05 μM. From the literature of electrochemical detection of cholestrol, various materials were applied for the detection. As far as our knowledge, metal oxide decorated reduced graphene oxide was not employed in the detection of Cholestrol. By comparing the common sensor characteristics like linear range and limit of detection, the present method gives better response which is listed in Table 2.

4.0 REPEATABILITY, REPRODUCIBILITY AND SELECTIVITY

The developed sensor was checked for the repeatability, reproducibility and the results were repeatable and reproducible with the deviation of ±2.78 % and ±2.21 % respectively. The sensor was tested for the selectivity with the presence of interferences like Uric acid, dopamine and ascorbic acid, the developed sensor is observed to be selective for cholestrol. The developed sensor was employed in detecting cholesterol in food samples like commercially available vanilla essence, vanilla flavored biscuit, vanilla flavored ice-cream and vanilla flavored cake mix. The detection was

TABLE 2. Comparison of different electrochemical methods for detection of Cholestrol

Reference	Electrode type	Limit of detection (μM)	Linear range (μM)
[35]	G/PVP/PANI nanocomposites	1	0.05-10
[36]	Graphene/GCE	0.056	0.6-48
[37]	MWCNT-PPy	1	0.4-6.5
[38]	Screen printed electrode	0.4	5-400
[39]	AuPd NP/Graphene/GCE	0.02	0.1-7 and 10-40
[40]	Au-f-MWCNT-PPy	2.88	2-8
[41]	AgNPs/Graphene nanosheets/GCE	0.332	2-100
[42]	Anode pre-treated BDDE	0.16	3.3-98
Present Work	rGO-TiO2/PPy-GCE	0.05	0.1-1 and 1-600

GCE-Glassy carbon electrode, AuPd NP- Gold Palladium Nanoparticles, CPE-Carbon paste electrode, Ag NPs- Silver Nanopartilces, poly (vinyl pyrrolidone) (PVP), polyaniline (PANI) multiwalled carbon nanotubes (MWCNT) and Polypyrrole (PPy).

successfully done and the results were validated using UV-Vis spectroscopy. The results are listed in Table 3.

TABLE 3. Real sample results with validation results using UV-Vis spectroscopy

Sample	Electrochemical		UV		Recovery (%)	
	μg/mL	RSD (%)	μg/mL	RSD(%)		
Biscuit	9.419	1.95	8.852	1.09	93.98	106.40
Pudding powder	35.511	1.71	29.95	0.606	84.34	118.56
Vanilla essence	39.703	1.84	36.271	2.42	91.355	108.12
Ice cream	10.122	3.75	12.13	1.37	119	83.36

5. CONCLUSION

A PPy modified Glassy carbon electrode was employed in detection of cholestrol. The modified electrode exhibited an excellent catalytic activity because of the presence of metal oxide. Selective and sensitive detection of cholestrol was obtained with wide linear range, low detective limit. The developed sensor *was successfully applied in detection of cholestrol in food samples like vanilla essence, vanilla flavored biscuits, ice cream and cake mix. The electrochemical results were validated using UV-visible spectrometry. The sensitivity was calculated for 0.1 μM to 1 μM and 1 μM to 600 μM was 61.665 and 0.1466 respectively.*

ACKNOWLEDGEMENTS

The authors are thankful to sophisticated test and instrumentation center, Cochin (Kerala),

Birla Institute of Technology, Hyderabad and Sri Ramakrishna Mission Vidyalaya College of Arts and Science, Coimbatore, TN, India. for providing instrumental facilities.

REFERENCES

1. Manley, C.; Mayer, J. Clinical Veterinary Advisor: Birds and Exotic Pets; Elsevier Inc.: Amsterdam, The Netherlands, (2012); pp. 613-614.
2. Motonaka, J.; Faulkner, L.R. Determination of Cholesterol and Cholesterol Ester with Novel Enzyme Microsensors. *Anal. Chem.* (1993), 65, 3258-3261.
3. Sekretaryova, A.N.; Beni, V.; Eriksson, M.; Karyakin, A.A.; Turner, A.P.F.; Vagin, M.Y. Cholesterol self-powered biosensor. *Anal. Chem.* (2014), 86, 9540-9547.
4. M. A. Paulazo and A. O. Sodero, "Analysis of cholesterol in mouse brain by HPLC with UV detection," *PLoS one*, vol. 15, no. 1, article e0228170, 2020.
5. H. I. Oh, T. S. Shin, and E. J. Chang, "Determination of cholesterol in milk and dairy products by high-performance liquid chromatography," *Asian-Australasian Journal of Animal Sciences*, vol. 14, no. 10, pp. 1465-1469, 2001.
6. K. Z. Liu, M. Shi, A. Man, T. C. Dembinski, and R. A. Shaw, "Quantitative determination of serum LDL cholesterol by near-infrared spectroscopy," *Vibrational Spectroscopy*, vol. 38, no. 1-2, pp. 203-208, 2005.V
7. J. Wang, Y. J. Geng, B. Guo et al., "Near-infrared spectroscopic characterization of human advanced atherosclerotic plaques," *Journal of the American College of Cardiology*, vol. 39, no. 8, (2002) pp. 1305-1313.
8. J. Chitra, M. Ghosh, and H. N. Mishra, "Rapid quantification of cholesterol in dairy powders using Fourier transform near infrared spectroscopy and chemometrics," *Food Control*, vol. 78, (2017), pp. 342-349.
9. T. Lin, L. Zhong, H. Chen et al., "A sensitive colorimetric assay for cholesterol based on the peroxidase-like activity of MoS_2 nanosheets," *Microchimica Acta*, vol. 184, no. 4, pp. 1233-1237, 2017.
10. X. Li, Z. Pu, and H. Zhou, "Synergistically enhanced peroxidase-like activity of Pd nanoparticles dispersed on CeO_2 nanotubes and their application in colorimetric sensing of sulfhydryl compounds," *Journal of Materials Science*, vol. 53, no. 19, pp. 13912-13923, 2018.
11. Y. Lia, Z. Kang, L. Kong et al., "MXene-Ti_3C_2/CuS nanocomposites: enhanced peroxidase-like activity and sensitive colorimetric cholesterol detection," *Materials Science & Engineering C*, vol. 104, (2019), article 110000.
12. A. K. Giri, C. Charan, A. Saha, V. K. Shahi, and A. B. Panda, "An amperometric cholesterol biosensor with excellent sensitivity and limit of detection based on an enzyme-immobilized microtubular ZnO@ZnS heterostructure," *Journal of Materials Chemistry A*, vol. 2, no. 40, (2014), pp. 16997-17004.
13. U. Saxena and A. B. Das, "Nanomaterials towards fabrication of cholesterol biosensors: key roles and design approaches," *Biosensor and Bioelectronic*, vol. 75, (2016), pp. 196-205.
14. M. Dervisevic, E. Çevik, M. ª enel, C. Nergiz, and M. F. Abasiyanik, "Amperometric cholesterol biosensor based on reconstituted cholesterol oxidase on boronic acid functional conducting polymers," *Journal of Electroanalytical Chemistry*, vol. 776, (2016), pp. 18-24.
15. F. Yildirimoðlu, F. Arslan, S. Çete, A. Yaº ar Preparation of a polypyrrole-polyvinylsulphonate composite film biosensor for determination of cholesterol based on entrapment of cholesterol oxidase Sensors, 9 (2009), 6435-6445.
16. M. Alagappan, Susan Immanuel, R. Sivasubramanian, A. Kandaswamy Development of cholesterol biosensor using Au nanoparticles decorated f-MWCNT covered with polypyrrole network, *Arabian Journal of Chemistry* 13 (2020), 2001-2010.

17. A. A. Ansari, A. Kaushik, P. R. Solanki, and B. D. Malhotra," Electrochemical cholesterol sensor based on tin oxidechitosannanobiocomposite film," *Electroanalysis,* vol. 8, (2009), pp. 965-972.

18. N. T. Nguyet, L. T. H. Yen, V. Y. Doan et al., "A label-free andhighly sensitive DNA biosensor based on the core-shell structuredCeO2-NR@Ppy nanocomposite for Salmonella detection," Materials Science & Engineering C, vol. 96, (2019), pp. 790-797.

19. A. Tiwari and S. Gong, "Electrochemical study of chitosan-SiO2-MWNT composite electrodes for the fabrication of cholesterol biosensors," *Electroanalysis,* vol. 20, no. 19, (2008), pp. 2119-2126.

20. A. Wisitsoraat, P. Sritongkham, C. Karuwan, D. Phokharatkul,T. Maturos, and A. Tuantranont, "Fast cholesterol detection using flow injection microfluidic device with functionalizedcarbon nanotubes based electrochemical sensor," *Biosensors and Bioelectronics,* 26, (2010), 1514-1520.

21. Si, P.; Ding, S.J.; Yuan, J.; Lou, X.W.; Kim, D.H. Hierarchically structured one-dimensional TiO2 for protein immobilization, direct electrochemistry, and mediator-free glucose sensing. ACS Nano (2011), 5, 7617-7626.

22. Chen, J.S.; Xu, L.; Xing, R.Q.; Song, J.; Song, H.W.; Liu, D.L.; Zhou, J. Electrospun three-dimensional porous CuO/TiO2 hierarchical nanocomposites electrode for nonenzymatic glucose biosensing. *Electrochem. Commun.* (2012), 20, 75-78.

23. He, M.Q.; Bao, L.L.; Sun, K.Y.; Zhao, D.X.; Li, W.B.; Xia, J.X.; Li, H.M. Synthesis of molecularly imprinted polypyrrole/titanium dioxide nanocomposites and its selective photocatalytic degradation of rhodamine B under visible light irradiation. *Express Polym. Lett.* (2014), 8, 850-861.

24. Bai, J.; Zhou, B.X. Titanium dioxide nanomaterials for sensor applications. *Chem. Rev.* (2014), 114, 10131-10176.

25. Yang, Q.; Long, M.; Tan, L.; Zhang, Y.; Ouyang, J.; Liu, P.; Tang, A.D. Helical TiO2 nanotube arrays modified by Cu-Cu2O with ultrahigh sensitivity for the nonenzymatic electro-oxidation of glucose. ACS Appl. *Mater. Interface* (2015), 7, 12719-12730.

26. Nilem Khaliq Muhammad Asim Rasheed Gihoon Cha Maaz Khan Shafqat Karim Patrik Schmuki GhafarAli Development of non-enzymatic cholesterol bio-sensor based on TiO_2 nanotubes decorated with Cu_2O nanoparticles Sensors and Actuators B: Chemical 302, (2020), 127200.

27. Singh K., Solanki, P.R., Basu, T. , Malhotra, B.D., Polypyrrole/multiwalled carbon nanotubes-based biosensor for cholesterol estimation Polymer Adv. Tech, 23 (2012)1084-1091.

28. Bettazzi F., Palchetti I., Sisalli S., Mascini M. A disposable electrochemical sensor for vanillin detection. *Anal. Chim. Acta.* 55592006) 134-138.

29. J. Fu, G. Kyzas, Z. Cai, E. Deliyanni, W. Liu and D. Zhao, *Chem. Eng. J.,* 335 (2018) 290-300.

30. W. Tang, G. Zeng, J. Gong, J. Liang, P. Xu, C. Zhang and B. Huang, *Sci. Total Environ.,* (2014), 1014-1027.

31. Cai, G.; Xu, Z.; Yang, M.; Tang, B.; Wang, X. Functionalization of cotton fabrics through thermal reduction of graphene oxide. *Appl. Surf. Sci.* 393 (2017), 441-448.

32. Qi Lai, Shifu Zhu, Xueping Luo, Min Zou, and Shuanghua Huang, Ultraviolet-visible spectroscopy of graphene oxides *AIP ADVANCES 2* (2012), 032146.

33. D. Li, M. B. Müller, S. Gilje, R. B. Kaner, and G. G. Wallace, Processable aqueous dispersions of graphene nanosheets," *Nature Nanotechnology,* 3 (2008), 101-105.

34. Liu, L., Luo, C., Xiong, J., Yang, Z., Zhang, Y., Cai, Y., & Gu, H. Reduced graphene oxide (rGO) decorated TiO_2 microspheres for visible-light photocatalytic reduction of Cr(VI). *Journal of Alloys and Compounds,* 690 (2017), 771-776.

35. Nipapan Ruecha, Ratthapol Rangkupan , Nadnudda Rodthongkum & Orawon Chailapakul Novel paper-based cholesterol biosensor using graphene/polyvinylpyrrolidone/polyaniline nanocomposite Biosensors and Bioelectronics, 52 (2014) 13–19.

36. Peng J., Hou C., Hu X. A graphene-based electrochemical sensor for sensitive detection of vanillin. *Int. J. Electrochem. Sci.* 7(2012), 1724-1733.

37. Alagappan,M., SusanImmanuel, Sivasubramanian, R., Kandaswamy,A., Development of cholesterol biosensor using Au nanoparticles decorated f-MWCNT covered with polypyrrole network, *Arabian Journal of Chemistry,* 13 (2020), 2001-2010.

38. Waliszewski K.N., Pardio V.T., Ovando S.L. A simple and rapid HPLC technique for vanillin determination in alcohol extract. *Food Chem.* 101 (2006), 1059–1062.

39. Huang L, Hou K, Jia X, Pan H, Du M Preparation of novel silver nanoplates/graphene composite and their application in vanillin electrochemical detection. *Mater Sci Eng C Mater Biol Appl.* 38 (2014), 39-45.

40. Yardım,Y., Gülcan, M., ª entürk, Z., Determination of vanillin in commercial food product by adsorptive stripping voltammetry using a boron-doped diamond electrode. Food Chem. 141 (2013), 1821-1827.

41. Krishnendu Pramanik, Priyabrata Sarkar et al., One Step Electrode Fabrication for Direct Electron Transfer Cholesterol Biosensor Based on Composite of Polypyrrole, Green Reduced Graphene Oxide and Cholesterol Oxidase, *Electroanalysis* (2018), 30, 1-13.

42. Nurul Akmaliah Dzulkurnain, Marliyana Mokhtar et al., A Review on Impedimetric and Voltammetric Analysis Based on Polypyrrole Conducting Polymers for Electrochemical Sensing Applications, *Polymers,* (2021), 13(16), 2728.

Received:

Accepted: